EUROPEAN ORGANIZATION FOR NUCLEAR RESEARCH

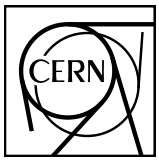

ALICE-PUBLIC-2021-001

ALICE luminosity determination for Pb–Pb collisions at $\sqrt{s_{\mathrm{NN}}} = 5.02$ TeV

ALICE Collaboration*

Abstract

Luminosity determination in ALICE is based on visible cross sections measured in van der Meer scans. In 2015 and 2018, the Large Hadron Collider provided Pb–Pb collisions at a centre-of-mass energy per nucleon pair of $\sqrt{s_{\mathrm{NN}}}$ = 5.02 TeV. Van der Meer scans were performed, in which the cross section was measured for two classes of visible interactions, based on particle detection in the ALICE luminometers: the Zero Degree Calorimeter (ZDC) and the V0 detector. This document describes the experimental set-up and summarises the main features of the analysis procedure. The resulting uncertainty on the ZDC-based (V0-based) luminosity measurement for the full sample is 2.3% (2.2%).

*See Appendix A for the list of collaboration members

1 Introduction

Luminosity determination in ALICE (A Large Ion Collider Experiment) [1] at the Large Hadron Collider (LHC) is based on visible cross sections measured in van der Meer (vdM) scans [2–4]. For collisions of lead ions (Pb–Pb), the visible cross section $\sigma_{\rm vis}$ seen by a detector (or set of detectors) with a given trigger condition has, in general, two components, one hadronic and one electromagnetic: $\sigma_{\rm vis} = \varepsilon_{\rm had}\sigma_{\rm had} + \varepsilon_{\rm EM}\sigma_{\rm EM}$, where $\sigma_{\rm had}$ and $\sigma_{\rm EM}$ are the hadronic and electromagnetic inelastic cross sections and $\varepsilon_{\rm had}$ and $\varepsilon_{\rm EM}$ are, respectively, the fractions of hadronic and electromagnetic inelastic events that satisfy the trigger condition. In the following, a class of events satisfying a given trigger condition will be referred to as a reference process. Once the reference-process cross section ($\sigma_{\rm vis}$) is measured, the luminosity at the ALICE interaction point (IP2) can be determined as the reference-process rate divided by $\sigma_{\rm vis}$. This procedure does not require a knowledge of $\varepsilon_{\rm had}$, $\varepsilon_{\rm EM}$.

In standard vdM scans, the two beams are moved across each other in the transverse directions x (horizontal) and y (vertical). The x and y scans are performed separately, the beams being head-on in the non-scanned direction. The measurement of the rate R of the reference process as a function of the beam separations Δx and Δy, defined as the distance between centroids of the beam bunches, allows one to determine the luminosity L for head-on collisions of a pair of bunches as

$$L = N_1 N_2 f_{\rm rev}/(h_x h_y), \tag{1}$$

where $f_{\rm rev}$ is the accelerator revolution frequency, N_1 and N_2 are the bunch intensities, defined as the number of particles in the bunch, and h_x and h_y are the effective widths of the beam overlap region in the two transverse directions (for head-on collisions). The effective widths h_x and h_y can be measured as the area under the rate curves $R(\Delta x, 0)$ and $R(0, \Delta y)$, respectively, each divided by the head-on rate $R(0,0)$. The cross section $\sigma_{\rm vis}$ for the chosen reference process is then

$$\sigma_{\rm vis} = R(0,0)/L. \tag{2}$$

The standard vdM scans are typically coupled with one or more length-scale calibration scans, whose aim is to determine the global conversion factor from the nominal (as dialled by the accelerator operator) to the actual beam displacement. In these scans, the two beams are kept at constant separation and moved in steps in the same direction, and the interaction vertex position is measured as a function of the nominal beam position.

The formalism of Eq. (1) assumes complete factorisation of the beam profiles in the two transverse directions, such that the beam overlap region is fully described by the product $h_x h_y$. Previous studies performed by ALICE [5–10] and other LHC experiments [11–14] have shown that the actual LHC bunch shapes can violate the factorisation assumption to a non-negligible level. Non-factorisation effects can be studied and quantified by measuring the luminous region parameters, via the distribution of interaction vertices, as a function of the beam separation.

During the so-called Run 2, in 2015 and 2018, the LHC provided Pb–Pb collisions at a centre-of-mass energy per nucleon pair $\sqrt{s_{\rm NN}} = 5.02$ TeV. The ALICE luminosity determination for these data samples is based on a vdM scan session[1] that took place on November 29, 2018, during the LHC fill labelled with number 7483. In this scan session, the cross section was measured for two independent reference processes.

[1] Two more vdM scan sessions, LHC fills 4690 and 7440, were not considered for this analysis. During fill 4690 (December 4, 2015) the LHC orbit feedback system, normally left off during vdM scans in order to not perturb the scan machinery, had to be left on due to beam instabilities; during fill 7440 (November 13, 2018) some of the quadrupole magnets determining the beam optics at IP2 had non-correct settings, leading to coupling between the two transverse directions. Due to the non trivial implications of these peculiar conditions on the vdM scan formalism and analysis, it was decided to base the luminosity normalisation on the vdM scan session of fill 7483 alone.

The rest of this document is organised as follows. Section 2 describes the detectors used for the measurement, along with the relevant machine parameters and the procedure adopted for the scan. Section 3 summarises the analysis procedure and presents the results and uncertainties for the visible cross section and the luminosity measurement. Finally, Sec. 4 presents a brief summary of the work.

2 Experimental set-up

In the vdM scan of fill 7483, the cross section was measured for two reference processes: one is based on the Zero Degree Calorimeter (ZDC), the other on the V0 detector. A detailed description of these detectors is given in [1], and their performance is discussed in [15, 16]. The ZDC system features two neutron calorimeters (ZNA, ZNC), located on opposite sides of IP2, each at a distance of 112.5 m along the beam line. It is completed by two proton calorimeters and two small electromagnetic calorimeters, not used for this measurement. The V0 detector consists of two hodoscopes, with 32 scintillator tiles each, located on opposite sides of the IP2, at distances of 340 cm (V0A) and 90 cm (V0C) along the beam axis, covering the pseudorapidity (η) ranges $2.8 < \eta < 5.1$ (V0A) and $-3.7 < \eta < -1.7$ (V0C). Note that the clockwise (anticlockwise) LHC beam 1 (2) travels from side A (C) to side C (A). The C side is the one hosting the ALICE muon arm [1].

The trigger condition used to define the ZDC-based visible cross section, called ZED in the following, requires a signal in at least one of the neutron calorimeters. Such a trigger condition is sensitive to both electromagnetic dissociation events with (single- or double-sided) neutron emission, and hadronic events [17–21]. The trigger condition for the V0-based visible cross section, called V0M in the following, requires the sum of signal amplitudes in all channels to be above some threshold; during the 2018 Pb–Pb data taking, the threshold was such that the $\sim 50\%$ most central hadronic events (and no electromagnetic events) were selected.

The analysis procedure uses, for the length-scale calibration and non-factorisation corrections, the parameters of the luminous region measured via the distribution of interaction vertices, determined with the ALICE Inner Tracking System (ITS [22]).

During the vdM scan session, each Pb beam consisted of 648 bunches, and 619 bunch pairs were made to collide at IP2. The minimum spacing between two consecutive bunches in each beam was 100 ns. The β^* value[2] at IP2 was 0.5 m. The nominal half vertical crossing angle of the two beams at IP2 was about -60 μrad, the minus sign indicating that the two beams exit the crossing region with negative y coordinate with respect to the beam axis[3]. The current in the ALICE solenoid (dipole) was 30 kA (6 kA), corresponding to a field strength of 0.5 T (0.7 T). The maximum beam separation during the scan was about 100 μm, corresponding to about six times the RMS of the transverse beam profile. The reference-process rates were recorded separately for each colliding bunch pair. Two pairs of horizontal and vertical scans were performed, to obtain two independent cross-section measurements per bunch pair. In addition, in order to provide additional input for non-factorisation studies, two diagonal scans were performed, where the beam separation was varied simultaneously in the two transverse directions. Finally, a set of length-scale calibration scans were performed.

The bunch intensities were of the order of $7–10\times10^7$ Pb ions per bunch. The bunch-intensity measurement is provided by the LHC instrumentation [23]: a DC current transformer (DCCT), measuring the total beam intensity, and a fast beam current transformer (fBCT), measuring the relative bunch intensities. For the relative bunch intensities, data from a second device, the ATLAS beam pick-up system

[2] The $\beta(z)$ function describes the single-particle motion and determines the variation of the beam envelope as a function of the coordinate along the beam orbit (z). The notation β^* denotes the value of the β function at the interaction point.

[3] ALICE uses a right-handed orthogonal Cartesian system whose origin is at the LHC Interaction Point 2 (IP2). The z axis is parallel to the mean beam direction at IP2 and points along the LHC Beam 2 (i.e. LHC anticlockwise). The x axis is horizontal and points approximately towards the centre of the LHC. The y axis is approximately vertical and points upwards.

(BPTX [24]) is also used. The measured beam intensity is corrected for the fraction of ghost and satellite charge. The radio-frequency (RF) configuration of the LHC is such that the accelerator orbit is divided in 3564 slots of 25 ns each. Each slot is further divided in ten buckets of 2.5 ns each. In nominally filled slots, the particle bunch is captured in the central bucket of the slot. Following the convention established in [25], the charge circulating outside of the nominally filled slots is referred to as ghost charge; the charge circulating within a nominally filled slot but not captured in the central bucket is referred to as satellite charge. A measurement of ghost charge is provided independently by the LHCb collaboration, via the rate of beam–gas collisions occurring in nominally empty bunch slots, as described in [11], and by the LHC Longitudinal Density Monitor (LDM), which measures synchrotron radiation photons emitted by the beams [26]. The LDM also provides a measurement of the satellite-charge fraction. For this fill, the combined ghost- and satellite-charge correction to the bunch intensity product (hence to the cross section) is about 13%. The total uncertainty on the bunch intensity is 0.8% and is obtained as the quadratic sum of the uncertainties on the total beam current normalisation from the DCCT (0.5%), on the relative bunch populations (0.2%), and on the ghost and satellite charge (0.6%).

3 Analysis and results

In previous studies, dedicated to luminosity determination in pp and p–Pb collisions [5–10], the trigger rates were corrected for background and pile-up effects, and the corrected rates plotted as a function of beam separation. The fit of the scan curves (separately for the x and y scans) yielded a measurement of $R(0,0)$, h_x, and h_y, which could be plugged directly into Eqs. 1 and 2 to determine $\sigma_{\rm vis}$. In the present analysis, the much smaller collision rate per colliding pair warranted a different approach, aimed to a better treatment of statistical uncertainties at very small numbers of counts. For each colliding bunch pair, the number of triggered events t_i and the number of sampled LHC orbits n_i at scan step i are used as inputs for a binomial likelihood fit:

$$\ln \mathscr{L} = \sum_i \left[t_i \ln P_i + (n_i - t_i) \ln (1 - P_i) \right] \tag{3}$$

where P_i is the probability of having a trigger in a bunch crossing, related to the mean number of triggers per bunch crossing μ_i by Poissonian statistics, $P_i = 1 - e^{-\mu_i}$. The quantity μ_i is modelled by the fit function, according to the following relation:

$$\mu_i = N_{1,i} N_{2,i} \frac{\sigma_{\rm vis}}{h_x h_y} f(\Delta x_i) g(\Delta y_i) + p_{{\rm s},i} + \tilde{p}_1 N_{1,i} + \tilde{p}_2 N_{2,i} + p_0, \tag{4}$$

where: $N_{1,i}$ and $N_{2,i}$ are the intensities of the two colliding bunches; Δx_i and Δy_i are the beam separations, corrected for beam–beam deflection [27, 28] and orbit drifts [29, 30]; f (g) parameterises the luminosity dependence on Δx_i (Δy_i); h_x (h_y) is the integral of f (g), divided by its peak value; $p_{{\rm s},i}$ is the probability that the trigger is fired by a collision between one of the two colliding bunches and a satellite of the other bunch; $\tilde{p}_1$ ($\tilde{p}_2$) is the probability that the trigger is fired by a beam–gas collision of a bunch of beam 1 (beam 2), normalised by the bunch intensity; p_0 is the probability that the trigger is fired in absence of colliding beams. Note that the visible cross section $\sigma_{\rm vis}$ is one of the fit parameters.

The functions $f(\Delta x)$ and $g(\Delta y)$ were chosen to have a Gaussian core with mean value and standard deviation as the only free parameters, the normalisation being constrained by Eqs. 1 and 2. In order to describe the scan-shape tails, the Gaussian function is modified for absolute separations larger than some value, chosen on the basis of fit quality and convergence considerations. For these scan steps, a separation-dependent offset is added to Δx_i or Δy_i, so that there is one additional fit parameter for each scan step beyond the core-tail transition point. Depending on the considered colliding bunch pair and scan, the transition point is located 1.3–2.5 standard deviations away from the peak, and the total number of tail parameters varies between 7 and 13. The function is constrained to be symmetric around the peak by using the same tail parameter for scan steps at opposite nominal separation.

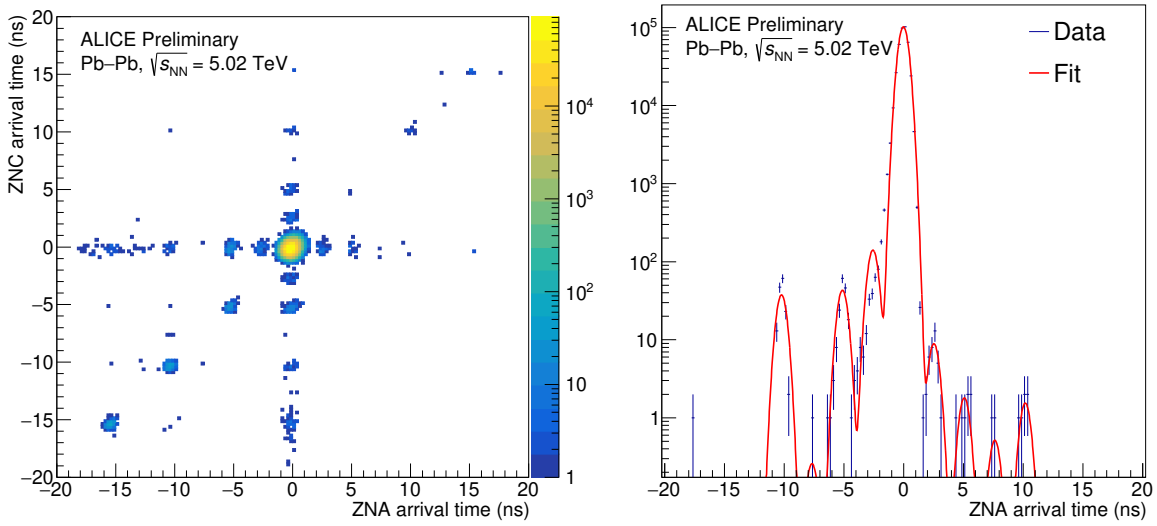

Fig. 1: (Colour online) Left: correlation between the arrival times of neutrons in ZNA and ZNC for events triggered by V0M. Right: arrival time on one of the two neutron calorimeters for ZED-triggered single-neutron events. The line shows a fit with a sum of Gaussian distributions. The nominal beam separation is zero for both figures.

The parameters p_0, $\tilde{p}_1$ and $\tilde{p}_2$ are estimated by means of an independent fit to the trigger rates in non-colliding and empty bunch slots. Owing to the minimum spacing of 100 ns between colliding bunches, the contribution to the trigger counts by after-pulses from a previous collision was found to be negligible for both signals. Hence, the empty bunch slots located immediately after colliding bunch slots, which are affected by background from after-pulses, were excluded from the fit. Because of the ZDC distance from the IP, the background induced on ZNA (ZNC) by beam–gas collisions of a bunch of beam 1(2) happening upstream of the calorimeter results in a signal that is earlier by 31 bunch slots (~ 750 ns) with respect to beam–beam collisions of the same bunch. For the filling scheme used in the vdM scan, this signal shows up in nominally empty bunch slots, which were excluded from the fit.

The separation-dependent contribution from main–satellite collisions $p_{{\rm s},i}$ is evaluated via the signal arrival time spectra in ZNA and ZNC. All events triggered by V0M have signals in both ZNA and ZNC. The two-dimensional distribution of arrival times in the two calorimeters for these events is shown in the left panel of Fig. 1. The satellite events are tagged by means of a square cut around the main–main peak position. The ZED trigger has a large contribution from events with single-neutron emission, so that most events have signal only in one calorimeter. For this sub-sample of ZED-triggered events, the estimation of the satellite contamination is based on the one-dimensional arrival time distributions in each of the ZNs, and the fraction of satellite collisions is obtained via a fit of the time distribution to a sum of Gaussian functions, with peak positions fixed to the values expected from the LHC radio-frequency structure (right panel of Fig. 1). Note that the signal from a single neutron emitted in a main–satellite collision has the same arrival time as that from a main–main collision if the neutron is emitted by an ion in the main bunch, while it is early or late if the neutron is emitted by an ion in the satellite bunch. Therefore, only half of the single neutrons from main–satellite collisions are identified as such, hence a correction factor of two is applied to the satellite-collision fractions obtained from the single-neutron event sample. Due to the dead time of the detector electronics, the timing information is only available for a fraction of the triggered events during the scan. Moreover, the size of the recorded sample does not allow for a bunch-by-bunch determination of satellite-collision fractions. In order to improve the statistical precision of the satellite estimation, the fit procedure is therefore extended with a joint likelihood maximisation, based on both timing and trigger data, at each separation step. Be S_i the number of events identified as main–satellite collisions in T_i acquired triggers, the joint binomial likelihood can be written

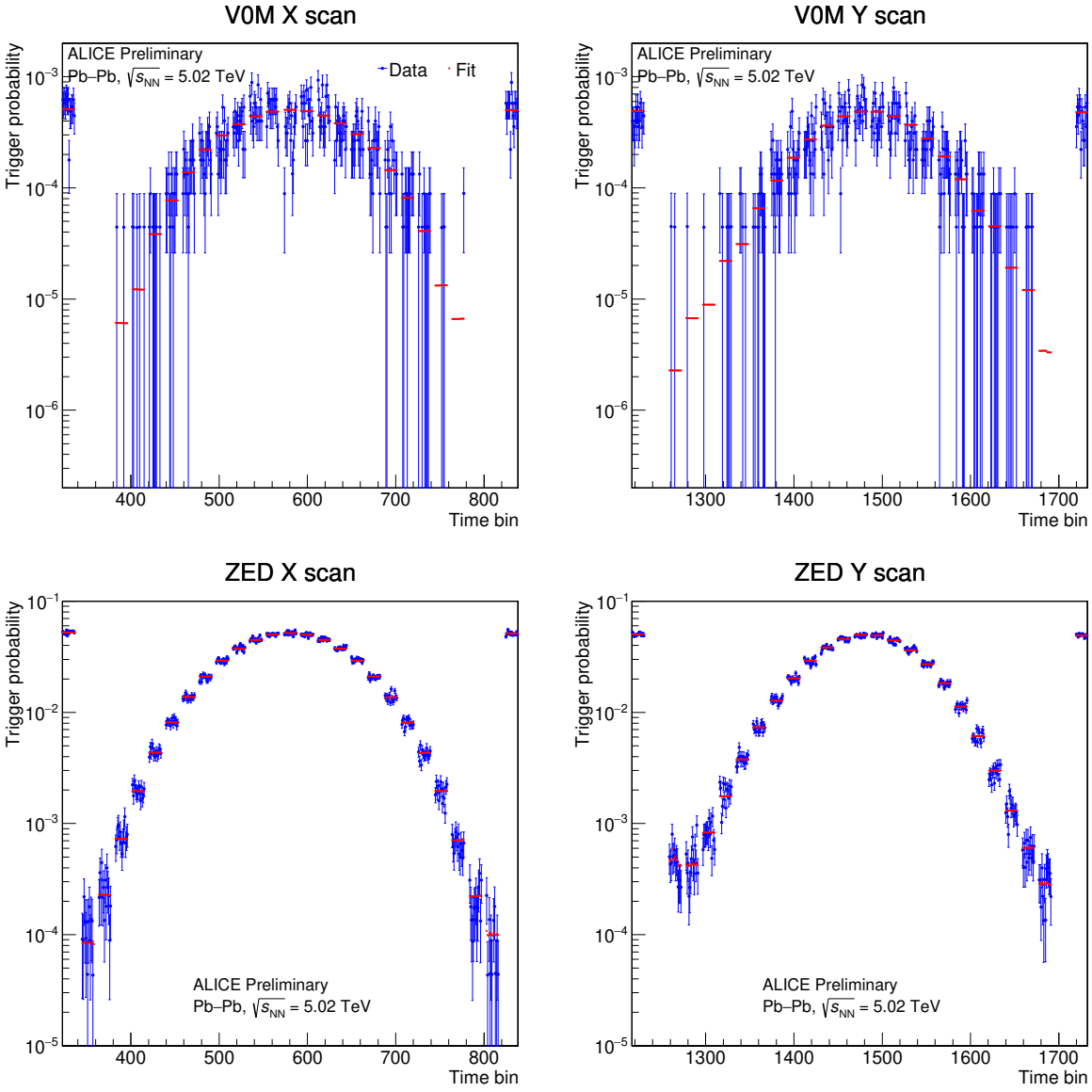

Fig. 2: (Colour online) V0M and ZED trigger probabilities per bunch crossing for a typical colliding bunch pair, as a function of time, during the first horizontal and vertical vdM scan. Each time bin corresponds to an acquisition window of $\sim$ 2 s. The uncertainties are statistical only. The fit expectation values are also shown. Time bins during which the beams are being displaced, not considered in the analysis, are not shown.

as

$$\ln \mathscr{L}_i = t_i \ln P_i + (n_i - t_i) \ln (1 - P_i) + S_i \ln \left(\frac{p_{\mathrm{s},i}}{P_i} \right) + (T_i - S_i) \ln \left(\frac{P_i - p_{\mathrm{s},i}}{P_i} \right). \quad (5)$$

The maximisation procedure determines the most probable value for $p_{\mathrm{s},i}$ for the measured values of n_i, t_i, T_i and S_i and the current expected P_i. The obtained $p_{\mathrm{s},i}$ is then fed into the global likelihood according to Eqs. 3 and 4.

In Fig. 2 the measured trigger probability per bunch crossing as a function of time during the vdM scan is shown for one pair of colliding bunches, together with the expectation from the fit. The quality of the fit is satisfactory, the values of χ^2/ndf being typically close to unity.

The V0M and ZED analyses provide independent estimates of the effective convolved beam widths h_x and h_y, via the fitted parameters of $f(\Delta x)$ and $g(\Delta y)$. The $h_x h_y$ products obtained in the V0M and in the

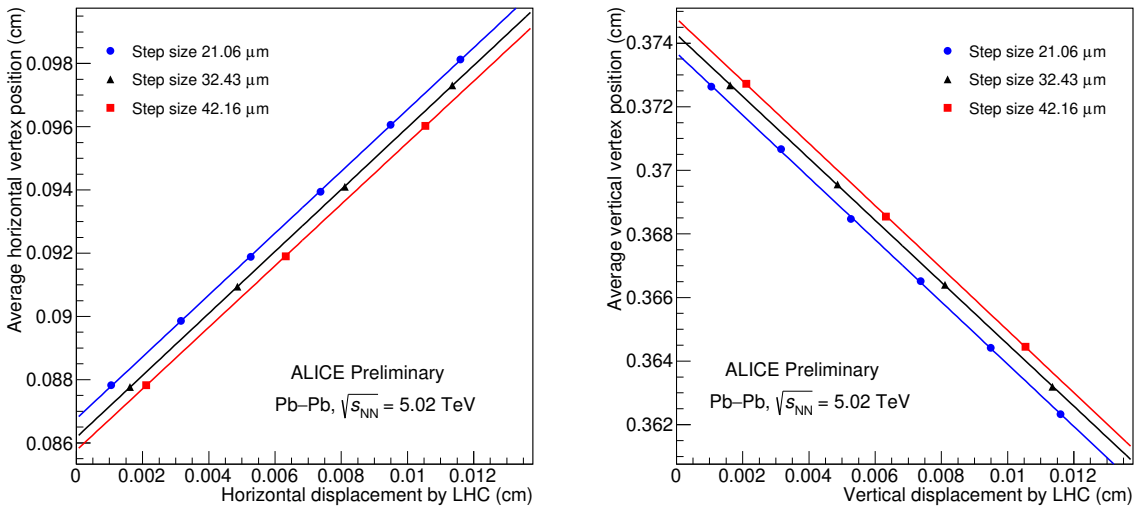

Fig. 3: (Colour online) Nominal versus measured displacements in the horizontal (left) and vertical (right) length-scale calibration scans. Data is represented by symbols, while a linear fit by the solid lines. The uncertainties are smaller than the symbol sizes. The blue (black, red) lines and solid circles (triangles, squares) correspond to a nominal displacement step size of 21.06 μm (32.43 μm, 42.16 μm).

ZED analysis are consistent within 0.13%, showing that detector-dependent effects are reasonably under control.

Three length-scale calibration scans were performed for each direction, with different displacement step size, in order to test a possible dependence on such a parameter. The horizontal (vertical) calibration factor is determined as the slope parameter of a linear fit to the measured horizontal (vertical) vertex displacement versus the nominal one, as illustrated in Fig. 3. The vertex position is determined using tracks reconstructed in the ITS. The resulting (multiplicative) correction factor to the fitted $\sigma_{\rm vis}$ is the product of the horizontal and vertical calibration factors, and was found to be 0.964 ± 0.010. The uncertainty is mostly systematic and accounts for deviations from the linear trend in the individual fits, for the dependence of the results on the displacement step size, and for the dependence of the results on the track and event selection criteria used in the vertex determination procedure.

The impact of non-factorisation effects is evaluated by simultaneously fitting the rates and the luminous-region parameters (positions, sizes, transverse tilt) during both the standard and the diagonal scans with a three-dimensional non-factorisable double-Gaussian model [6, 31], and computing the bias on the head-on luminosity with respect to a factorisable model. The resulting (multiplicative) correction factor to the fitted $\sigma_{\rm vis}$ is 1.011 ± 0.011, where an uncertainty as large as the correction is assigned to account for the non accurate description of some of the luminous-region parameters by the model.

The V0M and ZED cross sections measured for all colliding bunch pairs and scans are shown as a function of the product of bunch intensities N_1N_2 in Fig. 4. For both luminometers and scans, no significant dependence of $\sigma_{\rm vis}$ on N_1N_2 is observed. However, non-statistical fluctuations of the cross section are present in particular for ZED. In order to take these into account, a systematic uncertainty of $\sim 0.1\%$ (0.4%) for V0M (ZED) is assigned, computed as $\sqrt{\chi^2/ndf - 1}$ times the statistical uncertainty of the average cross section, where χ^2/ndf is obtained from the constant-value fits to the bunch-by-bunch cross sections shown in Fig. 4. The bunch-averaged cross sections measured in the two scans agree within 1%, which is considered as an additional systematic uncertainty. The measured visible cross sections, obtained by averaging the results from the two scans, are $\sigma_{\rm ZED}$ = 420.5 b $\pm$ 0.2 b (stat.) and

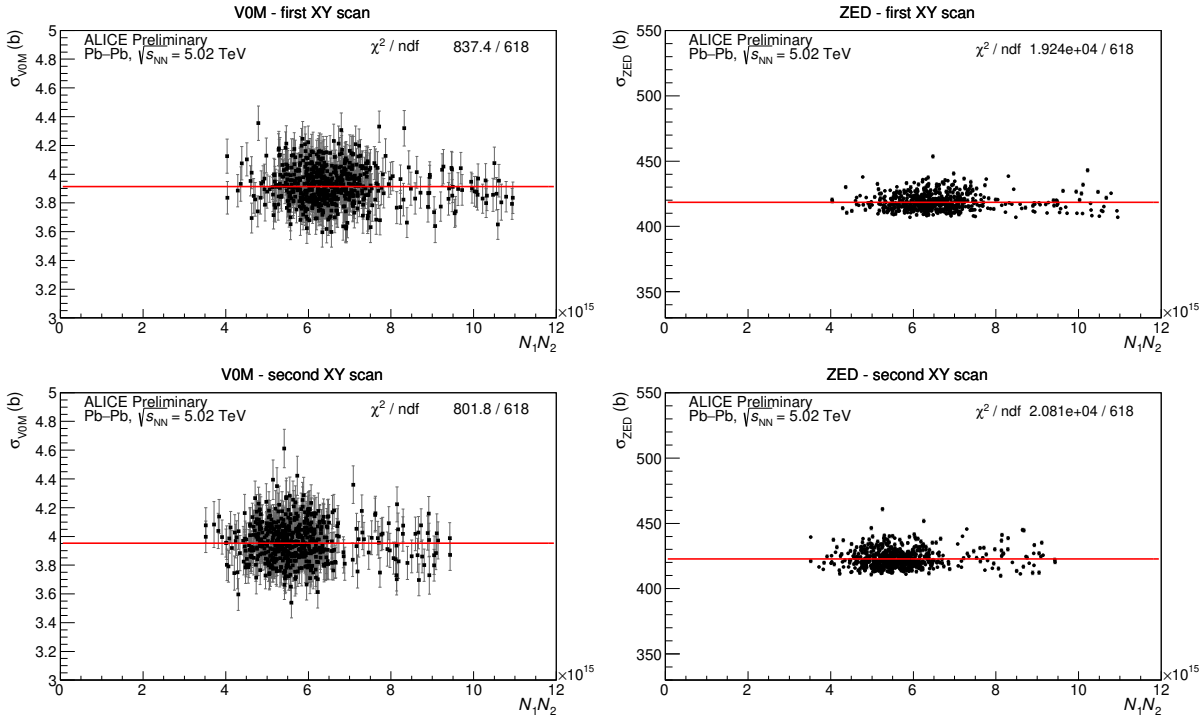

Fig. 4: (Colour online) V0M (left) and ZED (right) visible cross sections as a function of the product of the ion bunch intensities, for the first (top) and second vdM scan (bottom). Uncertainties are statistical only. The solid line represents a fit to a constant value.

$\sigma_{\mathrm{V0M}} = 3.933\ \mathrm{b} \pm 0.004\ \mathrm{b}$ (stat.).

The combined impact of the subtraction of background from beam–gas collisions, electronic noise, and satellite collisions on the final cross section is about 1% for V0M and 1.5% for ZED, largely dominated by satellite collisions. The systematic uncertainty on the background estimation from non-colliding and empty bunch slots is obtained by fitting the p_0, $\tilde{p}_1$ and $\tilde{p}_2$ parameters independently for each separation step, and computing the maximum difference with respect to the values obtained from a global fit to all separations. When the measured differences are propagated to the visible cross section, the resulting uncertainty is of the order of 0.1%. An additional systematic uncertainty arises from the fact that the subtraction of background from beam–satellite collisions is based on bunch-integrated timing data, neglecting differences in the bunch-by-bunch satellite fraction. In order to address this effect, the scan-step-averaged fraction of satellite collisions is evaluated for each colliding bunch pair, and found to fluctuate by about 40% (RMS). The satellite fractions S_i were therefore varied by this amount, resulting in a variation of the visible cross section by about 0.8% (0.5%) for ZED (V0M).

Possible non-linearities in the steering magnet behaviour during the scan, e.g. due to hysteresis, were considered as a source of systematic uncertainty. A preliminary hysteresis model[4] developed for the LHC was used to obtain an upper limit for the variations with respect to the nominal separation at each scan step; these variations, when propagated to the cross section, result in a 0.2% effect.

The uncertainty on the orbit drift correction was conservatively taken to be as large as the effect of the correction (0.15%). The uncertainty on the beam–beam deflection correction was evaluated by varying the input parameters to the deflection calculation within a reasonable range, as described in [6], and found to be less than 0.1%. The effect of distortions of the bunch shapes due to mutual interaction between the two beams was also evaluated, within the framework outlined in [28], and found to be less than 0.1%.

[4]M. Hofstettler and E. Todesco, 2020, presentations at the LHC Luminosity Calibration and Monitoring Working Group, November 16, and private communication, December 9.

The systematic uncertainty associated with the choice of the fitting strategy was evaluated by varying the range of beam separation described by the Gaussian core, by discarding the last scan step, where the satellite contribution is dominant, and by extracting the visible cross section from a simultaneous fit to all colliding bunch pairs instead of averaging the results from individual fits. The resulting uncertainty is 0.4%.

In order to test the stability and mutual consistency of the V0M and ZED calibration, the luminosities measured by the two devices throughout the 2015 and 2018 data-taking periods are compared. For each run[5] the trigger counts, integrated over colliding bunch slots, were corrected by subtracting the estimated beam–gas background, detector noise, and background from main–satellite collisions. The beam–gas background was estimated by means of the counts in non-colliding bunch slots, rescaled by the relative fractions of beam intensities. The contribution from detection noise was estimated via the counts in empty slots. The background from main–satellite collisions was estimated using the ZDC timing data. For each run, the ratio between the ZED- and V0M-based luminosities is computed from the corrected number of trigger counts $N_{\rm V0M}$ and $N_{\rm ZED}$ and from the total number of bunch crossings in the run $N_{\rm BC}$ as

$$\frac{L_{\rm ZED}}{L_{\rm V0M}} = \frac{\ln\left(1 - N_{\rm ZED}/N_{\rm BC}\right)\sigma_{\rm V0M}}{\ln\left(1 - N_{\rm V0M}/N_{\rm BC}\right)\sigma_{\rm ZED}}. \tag{6}$$

While the ZED trigger settings remained unchanged throughout the 2015 and 2018 data-taking periods, the threshold for the V0M trigger was different in 2015 and 2018. Furthermore, in 2018 it was slightly changed a few times during data-taking as the V0M-based centrality trigger was being tuned. For the data-taking periods with different threshold settings with respect to the vdM scan, the V0M trigger efficiency was measured relative to minimum bias collisions and the cross section rescaled by the ratio of the measured efficiency to that measured in the fill containing the van der Meer scans.

The luminosity ratio as a function of time and the distribution of the ratio over all runs, weighted with the run luminosity, is shown in Fig. 5. The mean quadratic difference of the ratio from unity is about 0.7% and is retained as a systematic uncertainty on the stability and mutual consistency of the luminosity calibration. When the analysis is restricted to the 2015 (2018) sample, the mean quadratic difference from unity amounts to 0.9% (0.5%).

In Table 1 a summary of the different contributions to the uncertainty on the visible cross section and the luminosity measurement is presented.

4 Conclusions

In 2015 and 2018, the ALICE Collaboration took data with Pb–Pb collisions at $\sqrt{s_{\rm NN}} = 5.02$ TeV. In order to provide a reference for the luminosity determination, vdM scans were performed and visible cross sections were measured for two processes, ZED and V0M, based on the ZDC and V0 detectors, respectively. The two detectors provide independent measurements of the luminosity, with a total uncertainty, for the full 2015+2018 sample, of 2.3% for the ZED and 2.2% for the V0M reference process. The quantitative contributions of the different sources of uncertainty considered for the visible cross section and the luminosity are shown in Table 1.

Acknowledgements

The ALICE Collaboration would like to thank all its engineers and technicians for their invaluable contributions to the construction of the experiment and the CERN accelerator teams for the outstanding

[5] In the ALICE nomenclature, a run is a set of data collected within a start and a stop of the data acquisition, under stable detector and trigger configurations. For the considered data-taking period, the duration of a run ranges from $\sim$ 5 minutes to $\sim$ 7 hours.

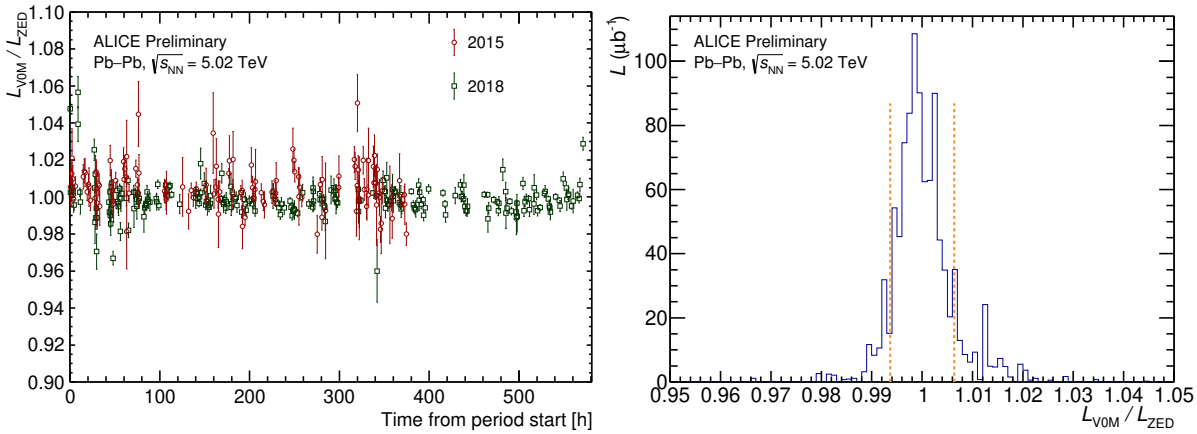

Fig. 5: (Colour online) Left: ratio of V0M and ZED luminosities calculated according to Eq. 6 as a function of time with respect to the beginning of the data-taking periods for 2015 (circles) and 2018 (squares). Right: distribution of the ratios for all runs (2015+2018); the dashed vertical lines are located at $L_{V0M}/L_{ZED} = 1 \pm \alpha$, where α is the mean quadratic difference from unity.

Source	Uncertainty (%) V0M | ZED
Statistical	0.09 | 0.04
Bunch intensity	0.8
$h_x h_y$ consistency (V0M vs ZED)	0.13
Length-scale calibration	1
Non-factorisation	1.1
Bunch-to-bunch consistency	0.1 | 0.4
Scan-to-scan consistency	1
Background subtraction	0.5 | 0.8
Magnetic non-linearities	0.2
Orbit drift	0.15
Beam–beam deflection and distortion	0.1
Fitting scheme	0.4
Total on visible cross section	2.1 | 2.2
Stability and consistency	0.7
Total on luminosity	2.2 | 2.3

Table 1: Relative uncertainties on the measurement of visible cross sections and luminosity in Pb–Pb collisions at $\sqrt{s_{NN}}$ = 5.02 TeV. The stability and consistency and the total luminosity uncertainties refer to the full Run 2 sample (2015+2018); uncertainties for the single periods are given in the text.

performance of the LHC complex. The ALICE Collaboration gratefully acknowledges the resources and support provided by all Grid centres and the Worldwide LHC Computing Grid (WLCG) collaboration. The ALICE Collaboration acknowledges the following funding agencies for their support in building and running the ALICE detector: A. I. Alikhanyan National Science Laboratory (Yerevan Physics Institute) Foundation (ANSL), State Committee of Science and World Federation of Scientists (WFS), Armenia; Austrian Academy of Sciences, Austrian Science Fund (FWF): [M 2467-N36] and Nationalstiftung für Forschung, Technologie und Entwicklung, Austria; Ministry of Communications and High Technologies, National Nuclear Research Center, Azerbaijan; Conselho Nacional de Desenvolvimento Científico e Tecnológico (CNPq), Financiadora de Estudos e Projetos (Finep), Fundação de Amparo à Pesquisa do Estado de São Paulo (FAPESP) and Universidade Federal do Rio Grande do Sul (UFRGS), Brazil; Ministry of Education of China (MOEC) , Ministry of Science & Technology of China (MSTC) and National Natural Science Foundation of China (NSFC), China; Ministry of Science and Education and Croatian Science Foundation, Croatia; Centro de Aplicaciones Tecnológicas y Desarrollo Nuclear (CEADEN), Cubaenergía, Cuba; Ministry of Education, Youth and Sports of the Czech Republic, Czech Republic; The Danish Council for Independent Research | Natural Sciences, the VILLUM FONDEN and Danish National Research Foundation (DNRF), Denmark; Helsinki Institute of Physics (HIP), Finland; Commissariat à l'Energie Atomique (CEA) and Institut National de Physique Nucléaire et de Physique des Particules (IN2P3) and Centre National de la Recherche Scientifique (CNRS), France; Bundesministerium für Bildung und Forschung (BMBF) and GSI Helmholtzzentrum für Schwerionenforschung GmbH, Germany; General Secretariat for Research and Technology, Ministry of Education, Research and Religions, Greece; National Research, Development and Innovation Office, Hungary; Department of Atomic Energy Government of India (DAE), Department of Science and Technology, Government of India (DST), University Grants Commission, Government of India (UGC) and Council of Scientific and Industrial Research (CSIR), India; Indonesian Institute of Science, Indonesia; Istituto Nazionale di Fisica Nucleare (INFN), Italy; Institute for Innovative Science and Technology , Nagasaki Institute of Applied Science (IIST), Japanese Ministry of Education, Culture, Sports, Science and Technology (MEXT) and Japan Society for the Promotion of Science (JSPS) KAKENHI, Japan; Consejo Nacional de Ciencia (CONACYT) y Tecnología, through Fondo de Cooperación Internacional en Ciencia y Tecnología (FONCICYT) and Dirección General de Asuntos del Personal Academico (DGAPA), Mexico; Nederlandse Organisatie voor Wetenschappelijk Onderzoek (NWO), Netherlands; The Research Council of Norway, Norway; Commission on Science and Technology for Sustainable Development in the South (COMSATS), Pakistan; Pontificia Universidad Católica del Perú, Peru; Ministry of Education and Science, National Science Centre and WUT ID-UB, Poland; Korea Institute of Science and Technology Information and National Research Foundation of Korea (NRF), Republic of Korea; Ministry of Education and Scientific Research, Institute of Atomic Physics and Ministry of Research and Innovation and Institute of Atomic Physics, Romania; Joint Institute for Nuclear Research (JINR), Ministry of Education and Science of the Russian Federation, National Research Centre Kurchatov Institute, Russian Science Foundation and Russian Foundation for Basic Research, Russia; Ministry of Education, Science, Research and Sport of the Slovak Republic, Slovakia; National Research Foundation of South Africa, South Africa; Swedish Research Council (VR) and Knut & Alice Wallenberg Foundation (KAW), Sweden; European Organization for Nuclear Research, Switzerland; Suranaree University of Technology (SUT), National Science and Technology Development Agency (NSDTA) and Office of the Higher Education Commission under NRU project of Thailand, Thailand; Turkish Atomic Energy Agency (TAEK), Turkey; National Academy of Sciences of Ukraine, Ukraine; Science and Technology Facilities Council (STFC), United Kingdom; National Science Foundation of the United States of America (NSF) and United States Department of Energy, Office of Nuclear Physics (DOE NP), United States of America.

References

[1] **ALICE** Collaboration, K. Aamodt *et al.*, "The ALICE experiment at the CERN LHC", *JINST* **3**

(2008) S08002.

[2] S. van der Meer, "Calibration of the effective beam height in the ISR", Tech. Rep. CERN-ISR-PO-68-31, CERN, 1968. http://cds.cern.ch/record/296752.

[3] V. Balagura, "Notes on van der Meer Scan for Absolute Luminosity Measurement", *Nucl. Instrum. Meth.* **A654** (2011) 634–638, arXiv:1103.1129 [physics.ins-det].

[4] P. Grafström and W. Kozanecki, "Luminosity determination at proton colliders", *Prog. Part. Nucl. Phys.* **81** (2015) 97–148.

[5] **ALICE** Collaboration, B. Abelev *et al.*, "Measurement of visible cross sections in proton-lead collisions at $\sqrt{s_{\rm NN}}$ = 5.02 TeV in van der Meer scans with the ALICE detector", *JINST* **9** no. 11, (2014) P11003, arXiv:1405.1849 [nucl-ex].

[6] **ALICE** Collaboration, J. Adam *et al.*, "ALICE luminosity determination for pp collisions at $\sqrt{s} = 13$ TeV", Tech. Rep. ALICE-PUBLIC-2016-002, CERN, 2016. https://cds.cern.ch/record/2160174/.

[7] **ALICE** Collaboration, S. Acharya *et al.*, "ALICE luminosity determination for pp collisions at $\sqrt{s} = 8$ TeV", Tech. Rep. ALICE-PUBLIC-2017-002, CERN, 2017. https://cds.cern.ch/record/2255216/.

[8] **ALICE** Collaboration, J. Adam *et al.*, "ALICE luminosity determination for pp collisions at $\sqrt{s} = 5$ TeV", Tech. Rep. ALICE-PUBLIC-2016-005, CERN, 2016. https://cds.cern.ch/record/2202638/.

[9] **ALICE** Collaboration, S. Acharya *et al.*, "ALICE 2017 luminosity determination for pp collisions at $\sqrt{s}$ = 5 TeV", Tech. Rep. ALICE-PUBLIC-2018-014, CERN, 2018. https://cds.cern.ch/record/2648933/.

[10] **ALICE** Collaboration, S. Acharya *et al.*, "ALICE luminosity determination for p-Pb collisions at $\sqrt{s_{\rm NN}}$ = 8.16 TeV", Tech. Rep. ALICE-PUBLIC-2018-002, CERN, 2018. https://cds.cern.ch/record/2314660/.

[11] **LHCb** Collaboration, R. Aaij *et al.*, "Precision luminosity measurements at LHCb", *JINST* **9** no. 12, (2014) P12005, arXiv:1410.0149 [hep-ex].

[12] **ATLAS** Collaboration, G. Aad *et al.*, "Improved luminosity determination in pp collisions at $\sqrt{s}$ = 7 TeV using the ATLAS detector at the LHC", *Eur. Phys. J.* **C73** no. 8, (2013) 2518, arXiv:1302.4393 [hep-ex].

[13] **ATLAS** Collaboration, M. Aaboud *et al.*, "Luminosity determination in pp collisions at $\sqrt{s}$ = 8 TeV using the ATLAS detector at the LHC", *Eur. Phys. J.* **C76** no. 12, (2016) 653, arXiv:1608.03953 [hep-ex].

[14] **CMS** Collaboration, "CMS Luminosity Based on Pixel Cluster Counting - Summer 2013 Update", Tech. Rep. CMS-PAS-LUM-13-001, CERN, 2013. https://cds.cern.ch/record/1598864.

[15] **ALICE** Collaboration, B. Abelev *et al.*, "Performance of the ALICE Experiment at the CERN LHC", *Int. J. Mod. Phys.* **A29** (2014) 1430044, arXiv:1402.4476 [nucl-ex].

[16] **ALICE** Collaboration, E. Abbas *et al.*, "Performance of the ALICE VZERO system", *JINST* **8** (2013) P10016, arXiv:1306.3130 [nucl-ex].

[17] A. J. Baltz, M. J. Rhoades-Brown, and J. Weneser, "Heavy-ion partial beam lifetimes due to Coulomb induced processes", *Physica Review E* **54** (1996) 4233.

[18] **ALICE** Collaboration, B. Abelev *et al.*, "Measurement of the Cross Section for Electromagnetic Dissociation with Neutron Emission in Pb-Pb Collisions at $\sqrt{s_{\rm NN}}$ = 2.76 TeV", *Phys. Rev. Lett.* **109** (2012) 252302, arXiv:1203.2436 [nucl-ex].

[19] I. A. Pshenichnov, J. P. Bondorf, I. N. Mishustin, A. Ventura, and S. Masetti, "Mutual heavy ion dissociation in peripheral collisions at ultrarelativistic energies", *Physical Review C* **64** no. 2, (Aug, 2001) 249031–2490319, 0101035. http://link.aps.org/doi/10.1103/PhysRevC.64.024903.

[20] I. Pshenichnov, "Electromagnetic excitation and fragmentation of ultrarelativistic nuclei", *Phys. Part. Nucl.* **42** no. 2, (Mar, 2011) 215–250. http://link.springer.com/10.1134/S1063779611020067.

[21] M. Broz, J. G. Contreras, and J. D. Tapia Takaki, "A generator of forward neutrons for ultra-peripheral collisions: $\mathbf{n}^{\mathbf{O}}_{\mathbf{O}}\mathbf{n}$", *Comput. Phys. Commun.* **253** (2020) 107181, arXiv:1908.08263 [nucl-th].

[22] **ALICE** Collaboration, K. Aamodt *et al.*, "Alignment of the ALICE Inner Tracking System with cosmic-ray tracks", *JINST* **5** (2010) P03003, arXiv:1001.0502 [physics.ins-det].

[23] J. J. Gras, D. Belohrad, M. Ludwig, P. Odier, and C. Barschel, "Optimization of the LHC beam current transformers for accurate luminosity determination", Tech. Rep. CERN-ATS-2011-063, CERN, 2011. http://cds.cern.ch/record/1379466.

[24] C. Ohm and T. Pauly, "The ATLAS beam pick-up based timing system", *Nucl. Instrum. Meth.* **A623** (2010) 558–560, arXiv:0905.3648 [physics.ins-det].

[25] A. Alici *et al.*, "Study of the LHC ghost charge and satellite bunches for luminosity calibration.", Tech. Rep. CERN-ATS-Note-2012-029 PERF, CERN, 2012. https://cds.cern.ch/record/1427728.

[26] A. Boccardi, E. Bravin, M. Ferro-Luzzi, S. Mazzoni, and M. Palm, "LHC Luminosity calibration using the Longitudinal Density Monitor", Tech. Rep. CERN-ATS-Note-2013-034 TECH, CERN, 2013. https://cds.cern.ch/record/1556087.

[27] W. Kozanecki, T. Pieloni, and J. Wenninger, "Observation of Beam-beam Deflections with LHC Orbit Data", Tech. Rep. CERN-ACC-NOTE-2013-0006, CERN, 2013. https://cds.cern.ch/record/1581723.

[28] V. Balagura, "Van der Meer Scan Luminosity Measurement and Beam-Beam Correction", arXiv:2012.07752 [hep-ex].

[29] D. Bishop, C. Boccard, E. Calvo-Giraldo, D. Cocq, L. Jensen, R. Jones, J. J. Savioz, and G. Waters, "The LHC Orbit and Trajectory System", Tech. Rep. CERN-AB-2003-057-BDI, 2003. https://cds.cern.ch/record/624190.

[30] J. Wenninger, "Dispersion Free Steering for YASP and dispersion correction for TI8", Tech. Rep. LHC-Performance-Note-005, CERN, 2009. http://cds.cern.ch/record/1156142.

[31] S. N. Webb, *Factorisation of beams in van der Meer scans and measurements of the ϕ^*_η distribution of $Z \to e^+e^-$ events in pp collisions at $\sqrt{s} = 8$ TeV with the ATLAS detector*. PhD thesis, Manchester U., 2015-06-01. https://inspirehep.net/record/1381312/files/CERN-THESIS-2015-054.pdf.

A The ALICE Collaboration

S. Acharya[142], D. Adamová[97], A. Adler[75], J. Adolfsson[82], G. Aglieri Rinella[35], M. Agnello[31], N. Agrawal[55], Z. Ahammed[142], S. Ahmad[16], S.U. Ahn[77], Z. Akbar[52], A. Akindinov[94], M. Al-Turany[109], D.S.D. Albuquerque[124], D. Aleksandrov[90], B. Alessandro[60], H.M. Alfanda[7], R. Alfaro Molina[72], B. Ali[16], Y. Ali[14], A. Alici[26], N. Alizadehvandchali[127], A. Alkin[35], J. Alme[21], T. Alt[69], L. Altenkamper[21], I. Altsybeev[115], M.N. Anaam[7], C. Andrei[49], D. Andreou[92], A. Andronic[145], V. Anguelov[106], T. Antičić[110], F. Antinori[58], P. Antonioli[55], C. Anuj[16], N. Apadula[81], L. Aphecetche[117], H. Appelshäuser[69], S. Arcelli[26], R. Arnaldi[60], I.C. Arsene[20], M. Arslandok[147,106], A. Augustinus[35], R. Averbeck[109], S. Aziz[79], M.D. Azmi[16], A. Badalà[57], Y.W. Baek[42], X. Bai[109], R. Bailhache[69], R. Bala[103], A. Balbino[31], A. Baldisseri[139], M. Ball[44], D. Banerjee[4], R. Barbera[27], L. Barioglio[107,25], M. Barlou[86], G.G. Barnaföldi[146], L.S. Barnby[96], V. Barret[136], C. Bartels[129], K. Barth[35], E. Bartsch[69], F. Baruffaldi[28], N. Bastid[136], S. Basu[82,144], G. Batigne[117], B. Batyunya[76], D. Bauri[50], J.L. Bazo Alba[114], I.G. Bearden[91], C. Beattie[147], I. Belikov[138], A.D.C. Bell Hechavarria[145], F. Bellini[35], R. Bellwied[127], S. Belokurova[115], V. Belyaev[95], G. Bencedi[70,146], S. Beole[25], A. Bercuci[49], Y. Berdnikov[100], A. Berdnikova[106], D. Berenyi[146], L. Bergmann[106], M.G. Besoiu[68], L. Betev[35], P.P. Bhaduri[142], A. Bhasin[103], I.R. Bhat[103], M.A. Bhat[4], B. Bhattacharjee[43], P. Bhattacharya[23], A. Bianchi[25], L. Bianchi[25], N. Bianchi[53], J. Bielčík[38], J. Bielčíková[97], A. Bilandzic[107], G. Biro[146], S. Biswas[4], J.T. Blair[121], D. Blau[90], M.B. Blidaru[109], C. Blume[69], G. Boca[29], F. Bock[98], A. Bogdanov[95], S. Boi[23], J. Bok[62], L. Boldizsár[146], A. Bolozdynya[95], M. Bombara[39], P.M. Bond[35], G. Bonomi[141], H. Borel[139], A. Borissov[83,95], H. Bossi[147], E. Botta[25], L. Bratrud[69], P. Braun-Munzinger[109], M. Bregant[123], M. Broz[38], G.E. Bruno[108,34], M.D. Buckland[129], D. Budnikov[111], H. Buesching[69], S. Bufalino[31], O. Bugnon[117], P. Buhler[116], Z. Buthelezi[73,133], J.B. Butt[14], S.A. Bysiak[120], D. Caffarri[92], A. Caliva[109], E. Calvo Villar[114], J.M.M. Camacho[122], R.S. Camacho[46], P. Camerini[24], F.D.M. Canedo[123], A.A. Capon[116], F. Carnesecchi[26], R. Caron[139], J. Castillo Castellanos[139], E.A.R. Casula[23], F. Catalano[31], C. Ceballos Sanchez[76], P. Chakraborty[50], S. Chandra[142], W. Chang[7], S. Chapeland[35], M. Chartier[129], S. Chattopadhyay[142], S. Chattopadhyay[112], A. Chauvin[23], T.G. Chavez[46], C. Cheshkov[137], B. Cheynis[137], V. Chibante Barroso[35], D.D. Chinellato[124], S. Cho[62], P. Chochula[35], P. Christakoglou[92], C.H. Christensen[91], P. Christiansen[82], T. Chujo[135], C. Cicalo[56], L. Cifarelli[26], F. Cindolo[55], M.R. Ciupek[109], G. Clai[II,55], J. Cleymans[126], F. Colamaria[54], J.S. Colburn[113], D. Colella[54,146], A. Collu[81], M. Colocci[35,26], M. Concas[III,60], G. Conesa Balbastre[80], Z. Conesa del Valle[79], G. Contin[24], J.G. Contreras[38], T.M. Cormier[98], P. Cortese[32], M.R. Cosentino[125], F. Costa[35], S. Costanza[29], P. Crochet[136], E. Cuautle[70], P. Cui[7], L. Cunqueiro[98], A. Dainese[58], F.P.A. Damas[117,139], M.C. Danisch[106], A. Danu[68], I. Das[112], P. Das[88], P. Das[4], S. Das[4], S. Dash[50], S. De[88], A. De Caro[30], G. de Cataldo[54], L. De Cilladi[25], J. de Cuveland[40], A. De Falco[23], D. De Gruttola[30], N. De Marco[60], C. De Martin[24], S. De Pasquale[30], S. Deb[51], H.F. Degenhardt[123], K.R. Deja[143], L. Dello Stritto[30], S. Delsanto[25], W. Deng[7], P. Dhankher[19], D. Di Bari[34], A. Di Mauro[35], R.A. Diaz[8], T. Dietel[126], Y. Ding[7], R. Divià[35], D.U. Dixit[19], Ø. Djuvsland[21], U. Dmitrieva[64], J. Do[62], A. Dobrin[68], B. Dönigus[69], O. Dordic[20], A.K. Dubey[142], A. Dubla[109,92], S. Dudi[102], M. Dukhishyam[88], P. Dupieux[136], T.M. Eder[145], R.J. Ehlers[98], V.N. Eikeland[21], D. Elia[54], B. Erazmus[117], F. Ercolessi[26], F. Erhardt[101], A. Erokhin[115], M.R. Ersdal[21], B. Espagnon[79], G. Eulisse[35], D. Evans[113], S. Evdokimov[93], L. Fabbietti[107], M. Faggin[28], J. Faivre[80], F. Fan[7], A. Fantoni[53], M. Fasel[98], P. Fecchio[31], A. Feliciello[60], G. Feofilov[115], A. Fernández Téllez[46], A. Ferrero[139], A. Ferretti[25], V.J.G. Feuillard[106], J. Figiel[120], S. Filchagin[111], D. Finogeev[64], F.M. Fionda[21], G. Fiorenza[54], F. Flor[127], A.N. Flores[121], S. Foertsch[73], P. Foka[109], S. Fokin[90], E. Fragiacomo[61], U. Fuchs[35], N. Funicello[30], C. Furget[80], A. Furs[64], J.J. Gaardhøje[91], M. Gagliardi[25], A.M. Gago[114], A. Gal[138], C.D. Galvan[122], P. Ganoti[86], C. Garabatos[109], J.R.A. Garcia[46], E. Garcia-Solis[10], K. Garg[117], C. Gargiulo[35], A. Garibli[89], K. Garner[145], P. Gasik[107], E.F. Gauger[121], M.B. Gay Ducati[71], M. Germain[117], J. Ghosh[112], P. Ghosh[142], S.K. Ghosh[4], M. Giacalone[26], P. Gianotti[53], P. Giubellino[109,60], P. Giubilato[28], A.M.C. Glaenzer[139], P. Glässel[106], V. Gonzalez[144], L.H. González-Trueba[72], S. Gorbunov[40], L. Görlich[120], S. Gotovac[36], V. Grabski[72], L.K. Graczykowski[143], K.L. Graham[113], L. Greiner[81], A. Grelli[63], C. Grigoras[35], V. Grigoriev[95], A. Grigoryan[I,1], S. Grigoryan[76,1], O.S. Groettvik[21], F. Grosa[60], J.F. Grosse-Oetringhaus[35], R. Grosso[109], R. Guernane[80], M. Guilbaud[117], M. Guittiere[117], K. Gulbrandsen[91], T. Gunji[134], A. Gupta[103], R. Gupta[103], I.B. Guzman[46], M.K. Habib[109], C. Hadjidakis[79], H. Hamagaki[84], G. Hamar[146], M. Hamid[7], R. Hannigan[121], M.R. Haque[143,88], A. Harlenderova[109], J.W. Harris[147], A. Harton[10], J.A. Hasenbichler[35], H. Hassan[98], D. Hatzifotiadou[55], P. Hauer[44], L.B. Havener[147], S. Hayashi[134], S.T. Heckel[107], E. Hellbär[69], H. Helstrup[37], T. Herman[38], E.G. Hernandez[46], G. Herrera Corral[9], F. Herrmann[145], K.F. Hetland[37], H. Hillemanns[35], C. Hills[129], B. Hippolyte[138], B. Hohlweger[92,107], J. Honermann[145], G.H. Hong[148], D. Horak[38], S. Hornung[109], R. Hosokawa[15], P. Hristov[35], C. Huang[79], C. Hughes[132], P. Huhn[69], T.J. Humanic[99], H. Hushnud[112], L.A. Husova[145], N. Hussain[43], D. Hutter[40], J.P. Iddon[35,129], R. Ilkaev[111], H. Ilyas[14], M. Inaba[135], G.M. Innocenti[35], M. Ippolitov[90], A. Isakov[38,97], M.S. Islam[112], M. Ivanov[109], V. Ivanov[100], V. Izucheev[93],

B. Jacak[81], N. Jacazio[35], P.M. Jacobs[81], S. Jadlovska[119], J. Jadlovsky[119], S. Jaelani[63], C. Jahnke[123], M.J. Jakubowska[143], M.A. Janik[143], T. Janson[75], M. Jercic[101], O. Jevons[113], M. Jin[127], F. Jonas[98,145], P.G. Jones[113], J. Jowett[35,109], J. Jung[69], M. Jung[69], A. Junique[35], A. Jusko[113], P. Kalinak[65], A. Kalweit[35], V. Kaplin[95], S. Kar[7], A. Karasu Uysal[78], D. Karatovic[101], O. Karavichev[64], T. Karavicheva[64], P. Karczmarczyk[143], E. Karpechev[64], A. Kazantsev[90], U. Kebschull[75], R. Keidel[48], M. Keil[35], B. Ketzer[44], Z. Khabanova[92], A.M. Khan[7], S. Khan[16], A. Khanzadeev[100], Y. Kharlov[93], A. Khatun[16], A. Khuntia[120], B. Kileng[37], B. Kim[62], D. Kim[148], D.J. Kim[128], E.J. Kim[74], J. Kim[148], J.S. Kim[42], J. Kim[106], J. Kim[148], J. Kim[74], M. Kim[106], S. Kim[18], T. Kim[148], S. Kirsch[69], I. Kisel[40], S. Kiselev[94], A. Kisiel[143], J.L. Klay[6], J. Klein[35], S. Klein[81], C. Klein-Bösing[145], M. Kleiner[69], T. Klemenz[107], A. Kluge[35], A.G. Knospe[127], C. Kobdaj[118], M.K. Köhler[106], T. Kollegger[109], A. Kondratyev[76], N. Kondratyeva[95], E. Kondratyuk[93], J. Konig[69], S.A. Konigstorfer[107], P.J. Konopka[2,35], G. Kornakov[143], S.D. Koryciak[2], L. Koska[119], O. Kovalenko[87], V. Kovalenko[115], M. Kowalski[120], I. Králik[65], A. Kravčáková[39], L. Kreis[109], M. Krivda[113,65], F. Krizek[97], K. Krizkova Gajdosova[38], M. Kroesen[106], M. Krüger[69], E. Kryshen[100], M. Krzewicki[40], V. Kučera[35], C. Kuhn[138], P.G. Kuijer[92], T. Kumaoka[135], L. Kumar[102], S. Kundu[88], P. Kurashvili[87], A. Kurepin[64], A.B. Kurepin[64], A. Kuryakin[111], S. Kushpil[97], J. Kvapil[113], M.J. Kweon[62], J.Y. Kwon[62], Y. Kwon[148], S.L. La Pointe[40], P. La Rocca[27], Y.S. Lai[81], A. Lakrathok[118], M. Lamanna[35], R. Langoy[131], K. Lapidus[35], P. Larionov[53], E. Laudi[35], L. Lautner[35], R. Lavicka[38], T. Lazareva[115], R. Lea[24], J. Lee[135], J. Lehrbach[40], R.C. Lemmon[96], I. León Monzón[122], E.D. Lesser[19], M. Lettrich[35], P. Lévai[146], X. Li[11], X.L. Li[7], J. Lien[131], R. Lietava[113], B. Lim[17], S.H. Lim[17], V. Lindenstruth[40], A. Lindner[49], C. Lippmann[109], A. Liu[19], J. Liu[129], I.M. Lofnes[21], V. Loginov[95], C. Loizides[98], P. Loncar[36], J.A. Lopez[106], X. Lopez[136], E. López Torres[8], J.R. Luhder[145], M. Lunardon[28], G. Luparello[61], Y.G. Ma[41], A. Maevskaya[64], M. Mager[35], T. Mahmoud[44], A. Maire[138], R.D. Majka[I,147], M. Malaev[100], Q.W. Malik[20], L. Malinina[IV,76], D. Mal'Kevich[94], N. Mallick[51], P. Malzacher[109], G. Mandaglio[33,57], V. Manko[90], F. Manso[136], V. Manzari[54], Y. Mao[7], J. Mareš[67], G.V. Margagliotti[24], A. Margotti[55], A. Marín[109], C. Markert[121], M. Marquard[69], N.A. Martin[106], P. Martinengo[35], J.L. Martinez[127], M.I. Martínez[46], G. Martínez García[117], S. Masciocchi[109], M. Masera[25], A. Masoni[56], L. Massacrier[79], A. Mastroserio[140,54], A.M. Mathis[107], O. Matonoha[82], P.F.T. Matuoka[123], A. Matyja[120], C. Mayer[120], A.L. Mazuecos[35], F. Mazzaschi[25], M. Mazzilli[35,54], M.A. Mazzoni[59], A.F. Mechler[69], F. Meddi[22], Y. Melikyan[64], A. Menchaca-Rocha[72], C. Mengke[28,7], E. Meninno[116,30], A.S. Menon[127], M. Meres[13], S. Mhlanga[126], Y. Miake[135], L. Micheletti[25], L.C. Migliorin[137], D.L. Mihaylov[107], K. Mikhaylov[76,94], A.N. Mishra[146,70], D. Miśkowiec[109], A. Modak[4], A.P. Mohanty[63], B. Mohanty[88], M. Mohisin Khan[16], Z. Moravcova[91], C. Mordasini[107], D.A. Moreira De Godoy[145], L.A.P. Moreno[46], I. Morozov[64], A. Morsch[35], T. Mrnjavac[35], V. Muccifora[53], E. Mudnic[36], D. Mühlheim[145], S. Muhuri[142], J.D. Mulligan[81], A. Mulliri[23], M.G. Munhoz[123], R.H. Munzer[69], H. Murakami[134], S. Murray[126], L. Musa[35], J. Musinsky[65], C.J. Myers[127], J.W. Myrcha[143], B. Naik[50], R. Nair[87], B.K. Nandi[50], R. Nania[55], E. Nappi[54], M.U. Naru[14], A.F. Nassirpour[82], C. Nattrass[132], S. Nazarenko[111], A. Neagu[20], L. Nellen[70], S.V. Nesbo[37], G. Neskovic[40], D. Nesterov[115], B.S. Nielsen[91], S. Nikolaev[90], S. Nikulin[90], V. Nikulin[100], F. Noferini[55], S. Noh[12], P. Nomokonov[76], J. Norman[129], N. Novitzky[135], P. Nowakowski[143], A. Nyanin[90], J. Nystrand[21], M. Ogino[84], A. Ohlson[82], J. Oleniacz[143], A.C. Oliveira Da Silva[132], M.H. Oliver[147], A. Onnerstad[128], C. Oppedisano[60], A. Ortiz Velasquez[70], T. Osako[47], A. Oskarsson[82], J. Otwinowski[120], K. Oyama[84], Y. Pachmayer[106], S. Padhan[50], D. Pagano[141], G. Paić[70], A. Palasciano[54], J. Pan[144], S. Panebianco[139], P. Pareek[142], J. Park[62], J.E. Parkkila[128], S. Parmar[102], S.P. Pathak[127], B. Paul[23], J. Pazzini[141], H. Pei[7], T. Peitzmann[63], X. Peng[7], L.G. Pereira[71], H. Pereira Da Costa[139], D. Peresunko[90], G.M. Perez[8], S. Perrin[139], Y. Pestov[5], V. Petráček[38], M. Petrovici[49], R.P. Pezzi[71], S. Piano[61], M. Pikna[13], P. Pillot[117], O. Pinazza[55,35], L. Pinsky[127], C. Pinto[27], S. Pisano[53], M. Płoskoń[81], M. Planinic[101], F. Pliquett[69], M.G. Poghosyan[98], B. Polichtchouk[93], N. Poljak[101], A. Pop[49], S. Porteboeuf-Houssais[136], J. Porter[81], V. Pozdniakov[76], S.K. Prasad[4], R. Preghenella[55], F. Prino[60], C.A. Pruneau[144], I. Pshenichnov[64], M. Puccio[35], S. Qiu[92], L. Quaglia[25], R.E. Quishpe[127], S. Ragoni[113], A. Rakotozafindrabe[139], L. Ramello[32], F. Rami[138], S.A.R. Ramirez[46], A.G.T. Ramos[34], R. Raniwala[104], S. Raniwala[104], S.S. Räsänen[45], R. Rath[51], I. Ravasenga[92], K.F. Read[98,132], A.R. Redelbach[40], K. Redlich[V,87], A. Rehman[21], P. Reichelt[69], F. Reidt[35], R. Renfordt[69], Z. Rescakova[39], K. Reygers[106], A. Riabov[100], V. Riabov[100], T. Richert[82,91], M. Richter[20], W. Riegler[35], F. Riggi[27], C. Ristea[68], S.P. Rode[51], M. Rodríguez Cahuantzi[46], K. Røed[20], R. Rogalev[93], E. Rogochaya[76], T.S. Rogoschinski[69], D. Rohr[35], D. Röhrich[21], P.F. Rojas[46], P.S. Rokita[143], F. Ronchetti[53], A. Rosano[33,57], E.D. Rosas[70], A. Rossi[58], A. Rotondi[29], A. Roy[51], P. Roy[112], N. Rubini[26], O.V. Rueda[82], R. Rui[24], B. Rumyantsev[76], A. Rustamov[89], E. Ryabinkin[90], Y. Ryabov[100], A. Rybicki[120], H. Rytkonen[128], W. Rzesa[143], O.A.M. Saarimaki[45], R. Sadek[117], S. Sadovsky[93], J. Saetre[21], K. Šafařík[38], S.K. Saha[142], S. Saha[88], B. Sahoo[50], P. Sahoo[50], R. Sahoo[51], S. Sahoo[66], D. Sahu[51], P.K. Sahu[66], J. Saini[142], S. Sakai[135], S. Sambyal[103], V. Samsonov[I,100,95], D. Sarkar[144], N. Sarkar[142], P. Sarma[43], V.M. Sarti[107], M.H.P. Sas[147,63], J. Schambach[98,121],

H.S. Scheid[69], C. Schiaua[49], R. Schicker[106], A. Schmah[106], C. Schmidt[109], H.R. Schmidt[105], M.O. Schmidt[106], M. Schmidt[105], N.V. Schmidt[98,69], A.R. Schmier[132], R. Schotter[138], J. Schukraft[35], Y. Schutz[138], K. Schwarz[109], K. Schweda[109], G. Scioli[26], E. Scomparin[60], J.E. Seger[15], Y. Sekiguchi[134], D. Sekihata[134], I. Selyuzhenkov[109,95], S. Senyukov[138], J.J. Seo[62], D. Serebryakov[64], L. Šerkšnytė[107], A. Sevcenco[68], A. Shabanov[64], A. Shabetai[117], R. Shahoyan[35], W. Shaikh[112], A. Shangaraev[93], A. Sharma[102], H. Sharma[120], M. Sharma[103], N. Sharma[102], S. Sharma[103], O. Sheibani[127], A.I. Sheikh[142], K. Shigaki[47], M. Shimomura[85], S. Shirinkin[94], Q. Shou[41], Y. Sibiriak[90], S. Siddhanta[56], T. Siemiarczuk[87], T.F. Silva[123], D. Silvermyr[82], G. Simatovic[92], G. Simonetti[35], B. Singh[107], R. Singh[88], R. Singh[103], R. Singh[51], V.K. Singh[142], V. Singhal[142], T. Sinha[112], B. Sitar[13], M. Sitta[32], T.B. Skaali[20], G. Skorodumovs[106], M. Slupecki[45], N. Smirnov[147], R.J.M. Snellings[63], C. Soncco[114], J. Song[127], A. Songmoolnak[118], F. Soramel[28], S. Sorensen[132], I. Sputowska[120], J. Stachel[106], I. Stan[68], P.J. Steffanic[132], S.F. Stiefelmaier[106], D. Stocco[117], M.M. Storetvedt[37], C.P. Stylianidis[92], A.A.P. Suaide[123], T. Sugitate[47], C. Suire[79], M. Suljic[35], R. Sultanov[94], M. Šumbera[97], V. Sumberia[103], S. Sumowidagdo[52], S. Swain[66], A. Szabo[13], I. Szarka[13], U. Tabassam[14], S.F. Taghavi[107], G. Taillepied[136], J. Takahashi[124], G.J. Tambave[21], S. Tang[136,7], Z. Tang[130], M. Tarhini[117], M.G. Tarzila[49], A. Tauro[35], G. Tejeda Muñoz[46], A. Telesca[35], L. Terlizzi[25], C. Terrevoli[127], G. Tersimonov[3], S. Thakur[142], D. Thomas[121], R. Tieulent[137], A. Tikhonov[64], A.R. Timmins[127], M. Tkacik[119], A. Toia[69], N. Topilskaya[64], M. Toppi[53], F. Torales-Acosta[19], S.R. Torres[38], A. Trifiró[33,57], S. Tripathy[55], T. Tripathy[50], S. Trogolo[28], G. Trombetta[34], V. Trubnikov[3], W.H. Trzaska[128], T.P. Trzcinski[143], B.A. Trzeciak[38], A. Tumkin[111], R. Turrisi[58], T.S. Tveter[20], K. Ullaland[21], E.N. Umaka[127], A. Uras[137], M. Urioni[141], G.L. Usai[23], M. Vala[39], N. Valle[29], S. Vallero[60], N. van der Kolk[63], L.V.R. van Doremalen[63], M. van Leeuwen[92], P. Vande Vyvre[35], D. Varga[146], Z. Varga[146], M. Varga-Kofarago[146], A. Vargas[46], M. Vasileiou[86], A. Vasiliev[90], O. Vázquez Doce[107], V. Vechernin[115], E. Vercellin[25], S. Vergara Limón[46], L. Vermunt[63], R. Vértesi[146], M. Verweij[63], L. Vickovic[36], Z. Vilakazi[133], O. Villalobos Baillie[113], G. Vino[54], A. Vinogradov[90], T. Virgili[30], V. Vislavicius[91], A. Vodopyanov[76], B. Volkel[35], M.A. Völkl[105], K. Voloshin[94], S.A. Voloshin[144], G. Volpe[34], B. von Haller[35], I. Vorobyev[107], D. Voscek[119], J. Vrláková[39], B. Wagner[21], M. Weber[116], A. Wegrzynek[35], S.C. Wenzel[35], J.P. Wessels[145], J. Wiechula[69], J. Wikne[20], G. Wilk[87], J. Wilkinson[109], G.A. Willems[145], E. Willsher[113], B. Windelband[106], M. Winn[139], W.E. Witt[132], J.R. Wright[121], Y. Wu[130], R. Xu[7], S. Yalcin[78], Y. Yamaguchi[47], K. Yamakawa[47], S. Yang[21], S. Yano[47,139], Z. Yin[7], H. Yokoyama[63], I.-K. Yoo[17], J.H. Yoon[62], S. Yuan[21], A. Yuncu[106], V. Yurchenko[3], V. Zaccolo[24], A. Zaman[14], C. Zampolli[35], H.J.C. Zanoli[63], N. Zardoshti[35], A. Zarochentsev[115], P. Závada[67], N. Zaviyalov[111], H. Zbroszczyk[143], M. Zhalov[100], S. Zhang[41], X. Zhang[7], Y. Zhang[130], V. Zherebchevskii[115], Y. Zhi[11], D. Zhou[7], Y. Zhou[91], J. Zhu[7,109], Y. Zhu[7], A. Zichichi[26], G. Zinovjev[3], N. Zurlo[141]

Affiliation notes

[I] Deceased
[II] Also at: Italian National Agency for New Technologies, Energy and Sustainable Economic Development (ENEA), Bologna, Italy
[III] Also at: Dipartimento DET del Politecnico di Torino, Turin, Italy
[IV] Also at: M.V. Lomonosov Moscow State University, D.V. Skobeltsyn Institute of Nuclear, Physics, Moscow, Russia
[V] Also at: Institute of Theoretical Physics, University of Wroclaw, Poland

Collaboration Institutes

[1] A.I. Alikhanyan National Science Laboratory (Yerevan Physics Institute) Foundation, Yerevan, Armenia
[2] AGH University of Science and Technology, Cracow, Poland
[3] Bogolyubov Institute for Theoretical Physics, National Academy of Sciences of Ukraine, Kiev, Ukraine
[4] Bose Institute, Department of Physics and Centre for Astroparticle Physics and Space Science (CAPSS), Kolkata, India
[5] Budker Institute for Nuclear Physics, Novosibirsk, Russia
[6] California Polytechnic State University, San Luis Obispo, California, United States
[7] Central China Normal University, Wuhan, China
[8] Centro de Aplicaciones Tecnológicas y Desarrollo Nuclear (CEADEN), Havana, Cuba
[9] Centro de Investigación y de Estudios Avanzados (CINVESTAV), Mexico City and Mérida, Mexico
[10] Chicago State University, Chicago, Illinois, United States
[11] China Institute of Atomic Energy, Beijing, China

[12] Chungbuk National University, Cheongju, Republic of Korea
[13] Comenius University Bratislava, Faculty of Mathematics, Physics and Informatics, Bratislava, Slovakia
[14] COMSATS University Islamabad, Islamabad, Pakistan
[15] Creighton University, Omaha, Nebraska, United States
[16] Department of Physics, Aligarh Muslim University, Aligarh, India
[17] Department of Physics, Pusan National University, Pusan, Republic of Korea
[18] Department of Physics, Sejong University, Seoul, Republic of Korea
[19] Department of Physics, University of California, Berkeley, California, United States
[20] Department of Physics, University of Oslo, Oslo, Norway
[21] Department of Physics and Technology, University of Bergen, Bergen, Norway
[22] Dipartimento di Fisica dell'Università 'La Sapienza' and Sezione INFN, Rome, Italy
[23] Dipartimento di Fisica dell'Università and Sezione INFN, Cagliari, Italy
[24] Dipartimento di Fisica dell'Università and Sezione INFN, Trieste, Italy
[25] Dipartimento di Fisica dell'Università and Sezione INFN, Turin, Italy
[26] Dipartimento di Fisica e Astronomia dell'Università and Sezione INFN, Bologna, Italy
[27] Dipartimento di Fisica e Astronomia dell'Università and Sezione INFN, Catania, Italy
[28] Dipartimento di Fisica e Astronomia dell'Università and Sezione INFN, Padova, Italy
[29] Dipartimento di Fisica e Nucleare e Teorica, Università di Pavia and Sezione INFN, Pavia, Italy
[30] Dipartimento di Fisica 'E.R. Caianiello' dell'Università and Gruppo Collegato INFN, Salerno, Italy
[31] Dipartimento DISAT del Politecnico and Sezione INFN, Turin, Italy
[32] Dipartimento di Scienze e Innovazione Tecnologica dell'Università del Piemonte Orientale and INFN Sezione di Torino, Alessandria, Italy
[33] Dipartimento di Scienze MIFT, Università di Messina, Messina, Italy
[34] Dipartimento Interateneo di Fisica 'M. Merlin' and Sezione INFN, Bari, Italy
[35] European Organization for Nuclear Research (CERN), Geneva, Switzerland
[36] Faculty of Electrical Engineering, Mechanical Engineering and Naval Architecture, University of Split, Split, Croatia
[37] Faculty of Engineering and Science, Western Norway University of Applied Sciences, Bergen, Norway
[38] Faculty of Nuclear Sciences and Physical Engineering, Czech Technical University in Prague, Prague, Czech Republic
[39] Faculty of Science, P.J. Šafárik University, Košice, Slovakia
[40] Frankfurt Institute for Advanced Studies, Johann Wolfgang Goethe-Universität Frankfurt, Frankfurt, Germany
[41] Fudan University, Shanghai, China
[42] Gangneung-Wonju National University, Gangneung, Republic of Korea
[43] Gauhati University, Department of Physics, Guwahati, India
[44] Helmholtz-Institut für Strahlen- und Kernphysik, Rheinische Friedrich-Wilhelms-Universität Bonn, Bonn, Germany
[45] Helsinki Institute of Physics (HIP), Helsinki, Finland
[46] High Energy Physics Group, Universidad Autónoma de Puebla, Puebla, Mexico
[47] Hiroshima University, Hiroshima, Japan
[48] Hochschule Worms, Zentrum für Technologietransfer und Telekommunikation (ZTT), Worms, Germany
[49] Horia Hulubei National Institute of Physics and Nuclear Engineering, Bucharest, Romania
[50] Indian Institute of Technology Bombay (IIT), Mumbai, India
[51] Indian Institute of Technology Indore, Indore, India
[52] Indonesian Institute of Sciences, Jakarta, Indonesia
[53] INFN, Laboratori Nazionali di Frascati, Frascati, Italy
[54] INFN, Sezione di Bari, Bari, Italy
[55] INFN, Sezione di Bologna, Bologna, Italy
[56] INFN, Sezione di Cagliari, Cagliari, Italy
[57] INFN, Sezione di Catania, Catania, Italy
[58] INFN, Sezione di Padova, Padova, Italy
[59] INFN, Sezione di Roma, Rome, Italy
[60] INFN, Sezione di Torino, Turin, Italy
[61] INFN, Sezione di Trieste, Trieste, Italy
[62] Inha University, Incheon, Republic of Korea
[63] Institute for Gravitational and Subatomic Physics (GRASP), Utrecht University/Nikhef, Utrecht, Netherlands

[64] Institute for Nuclear Research, Academy of Sciences, Moscow, Russia
[65] Institute of Experimental Physics, Slovak Academy of Sciences, Košice, Slovakia
[66] Institute of Physics, Homi Bhabha National Institute, Bhubaneswar, India
[67] Institute of Physics of the Czech Academy of Sciences, Prague, Czech Republic
[68] Institute of Space Science (ISS), Bucharest, Romania
[69] Institut für Kernphysik, Johann Wolfgang Goethe-Universität Frankfurt, Frankfurt, Germany
[70] Instituto de Ciencias Nucleares, Universidad Nacional Autónoma de México, Mexico City, Mexico
[71] Instituto de Física, Universidade Federal do Rio Grande do Sul (UFRGS), Porto Alegre, Brazil
[72] Instituto de Física, Universidad Nacional Autónoma de México, Mexico City, Mexico
[73] iThemba LABS, National Research Foundation, Somerset West, South Africa
[74] Jeonbuk National University, Jeonju, Republic of Korea
[75] Johann-Wolfgang-Goethe Universität Frankfurt Institut für Informatik, Fachbereich Informatik und Mathematik, Frankfurt, Germany
[76] Joint Institute for Nuclear Research (JINR), Dubna, Russia
[77] Korea Institute of Science and Technology Information, Daejeon, Republic of Korea
[78] KTO Karatay University, Konya, Turkey
[79] Laboratoire de Physique des 2 Infinis, Irène Joliot-Curie, Orsay, France
[80] Laboratoire de Physique Subatomique et de Cosmologie, Université Grenoble-Alpes, CNRS-IN2P3, Grenoble, France
[81] Lawrence Berkeley National Laboratory, Berkeley, California, United States
[82] Lund University Department of Physics, Division of Particle Physics, Lund, Sweden
[83] Moscow Institute for Physics and Technology, Moscow, Russia
[84] Nagasaki Institute of Applied Science, Nagasaki, Japan
[85] Nara Women's University (NWU), Nara, Japan
[86] National and Kapodistrian University of Athens, School of Science, Department of Physics , Athens, Greece
[87] National Centre for Nuclear Research, Warsaw, Poland
[88] National Institute of Science Education and Research, Homi Bhabha National Institute, Jatni, India
[89] National Nuclear Research Center, Baku, Azerbaijan
[90] National Research Centre Kurchatov Institute, Moscow, Russia
[91] Niels Bohr Institute, University of Copenhagen, Copenhagen, Denmark
[92] Nikhef, National institute for subatomic physics, Amsterdam, Netherlands
[93] NRC Kurchatov Institute IHEP, Protvino, Russia
[94] NRC «Kurchatov»Institute - ITEP, Moscow, Russia
[95] NRNU Moscow Engineering Physics Institute, Moscow, Russia
[96] Nuclear Physics Group, STFC Daresbury Laboratory, Daresbury, United Kingdom
[97] Nuclear Physics Institute of the Czech Academy of Sciences, Řež u Prahy, Czech Republic
[98] Oak Ridge National Laboratory, Oak Ridge, Tennessee, United States
[99] Ohio State University, Columbus, Ohio, United States
[100] Petersburg Nuclear Physics Institute, Gatchina, Russia
[101] Physics department, Faculty of science, University of Zagreb, Zagreb, Croatia
[102] Physics Department, Panjab University, Chandigarh, India
[103] Physics Department, University of Jammu, Jammu, India
[104] Physics Department, University of Rajasthan, Jaipur, India
[105] Physikalisches Institut, Eberhard-Karls-Universität Tübingen, Tübingen, Germany
[106] Physikalisches Institut, Ruprecht-Karls-Universität Heidelberg, Heidelberg, Germany
[107] Physik Department, Technische Universität München, Munich, Germany
[108] Politecnico di Bari and Sezione INFN, Bari, Italy
[109] Research Division and ExtreMe Matter Institute EMMI, GSI Helmholtzzentrum für Schwerionenforschung GmbH, Darmstadt, Germany
[110] Rudjer Bošković Institute, Zagreb, Croatia
[111] Russian Federal Nuclear Center (VNIIEF), Sarov, Russia
[112] Saha Institute of Nuclear Physics, Homi Bhabha National Institute, Kolkata, India
[113] School of Physics and Astronomy, University of Birmingham, Birmingham, United Kingdom
[114] Sección Física, Departamento de Ciencias, Pontificia Universidad Católica del Perú, Lima, Peru
[115] St. Petersburg State University, St. Petersburg, Russia
[116] Stefan Meyer Institut für Subatomare Physik (SMI), Vienna, Austria

[117] SUBATECH, IMT Atlantique, Université de Nantes, CNRS-IN2P3, Nantes, France
[118] Suranaree University of Technology, Nakhon Ratchasima, Thailand
[119] Technical University of Košice, Košice, Slovakia
[120] The Henryk Niewodniczanski Institute of Nuclear Physics, Polish Academy of Sciences, Cracow, Poland
[121] The University of Texas at Austin, Austin, Texas, United States
[122] Universidad Autónoma de Sinaloa, Culiacán, Mexico
[123] Universidade de São Paulo (USP), São Paulo, Brazil
[124] Universidade Estadual de Campinas (UNICAMP), Campinas, Brazil
[125] Universidade Federal do ABC, Santo Andre, Brazil
[126] University of Cape Town, Cape Town, South Africa
[127] University of Houston, Houston, Texas, United States
[128] University of Jyväskylä, Jyväskylä, Finland
[129] University of Liverpool, Liverpool, United Kingdom
[130] University of Science and Technology of China, Hefei, China
[131] University of South-Eastern Norway, Tonsberg, Norway
[132] University of Tennessee, Knoxville, Tennessee, United States
[133] University of the Witwatersrand, Johannesburg, South Africa
[134] University of Tokyo, Tokyo, Japan
[135] University of Tsukuba, Tsukuba, Japan
[136] Université Clermont Auvergne, CNRS/IN2P3, LPC, Clermont-Ferrand, France
[137] Université de Lyon, CNRS/IN2P3, Institut de Physique des 2 Infinis de Lyon , Lyon, France
[138] Université de Strasbourg, CNRS, IPHC UMR 7178, F-67000 Strasbourg, France, Strasbourg, France
[139] Université Paris-Saclay Centre d'Etudes de Saclay (CEA), IRFU, Départment de Physique Nucléaire (DPhN), Saclay, France
[140] Università degli Studi di Foggia, Foggia, Italy
[141] Università di Brescia and Sezione INFN, Brescia, Italy
[142] Variable Energy Cyclotron Centre, Homi Bhabha National Institute, Kolkata, India
[143] Warsaw University of Technology, Warsaw, Poland
[144] Wayne State University, Detroit, Michigan, United States
[145] Westfälische Wilhelms-Universität Münster, Institut für Kernphysik, Münster, Germany
[146] Wigner Research Centre for Physics, Budapest, Hungary
[147] Yale University, New Haven, Connecticut, United States
[148] Yonsei University, Seoul, Republic of Korea